

# STUDY TO INVESTIGATE THE EFFECTS OF IONIZING RADIATION ON TRANSISTOR SURFACES

Contract NAS 8-20135

FOURTH QUARTERLY REPORT  
FOR THE PERIOD ENDED JUNE 30, 1966

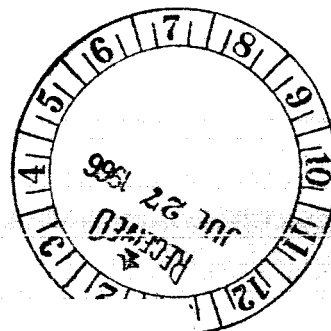
GPO PRICE \$ \_\_\_\_\_

CFSTI PRICE(S) \$ \_\_\_\_\_

Hard copy (HC) 3.00

Microfiche (MF) 1.50

ff 653 July 65



FACILITY FORM 802

**N66 37545**

(ACCESSION NUMBER)

54

(PAGES)

CP-78352

(NASA CR OR TMX OR AD NUMBER)

(THRU)

(CODE)

09

(CATEGORY)

**RESEARCH LABORATORIES DIVISION**  
**SOUTHFIELD, MICHIGAN**

**STUDY TO INVESTIGATE THE EFFECTS OF  
IONIZING RADIATION ON TRANSISTOR SURFACES**

**Contract NAS 8-20135**

**FOURTH QUARTERLY REPORT  
FOR THE PERIOD ENDED JUNE 30, 1966**

**July 15, 1966**

National Aeronautics and Space Administration  
George C. Marshall Space Flight Center  
Huntsville, Alabama 35812, Attn: PR - EC

The Bendix Corporation  
Research Laboratories Division  
Southfield, Michigan

Prepared by: Richard J. Sweet  
Richard J. Sweet

David L. Nelson  
David L. Nelson

Approved by: Donald J. Niehaus  
Donald J. Niehaus

TABLE OF CONTENTS

	<u>Page</u>
SECTION 1 - INTRODUCTION AND SUMMARY	1
SECTION 2 - FOURTH QUARTER TESTS	2
2.1 Phase I, Test 11--Vacuum Test	2
2.2 Phase II Tests	6
SECTION 3 - FURTHER ACTION REQUIRED	14

# LIST OF ILLUSTRATIONS

<u>Figure No.</u>	<u>Title</u>	<u>Page</u>
1	Ultrahigh Vacuum Envelopes for Irradiating Transistors	3
2	$1/h_{FE}$ and $I_{CBO}$ Versus Dose for Normal and Evacuated Ambients on Devices 36 and 40	5
3	$1/h_{FE}$ and $I_{CBO}$ Versus Dose for Two Cycles of Test II-1	8
4	Exponential Slope Constant and Base Emitter Capacity as a Function of Irradiation Time-- Devices 8 and 15	12

<u>Table No.</u>		
1	Vacuum-Irradiation Test for Phase I	4
2	Phase II Tests	7
3	Slope Constants for n-p-n and p-n-p Devices as a Function of Dose	10

## FOREWORD

The program whose status is described in this report is being performed for NASA, Marshall Space Flight Center, Astrionics Laboratory, for the purpose of delineating the effects of ionizing radiation on transistor surfaces. The work involves identifying and characterizing the mechanisms producing the effects, establishing models which describe the physical phenomena, developing nondestructive screening techniques which enable separating transistors with good immunity to radiation surface effects from those with poor immunity, and evaluating which, if any, surface treatments or manufacturing processes lead to a minimum of ionizing radiation surface effects.

The experimental portion of the program is conducted with 150 kV X-rays as the source of ionizing radiation. This radiation source is energetic enough to penetrate the transistor can and produce surface ionization, but not energetic enough to produce bulk transistor damage which would unduly complicate the results by combining surface and bulk damage. Extensive use is made of low current surface behavior which accentuates the phenomena, and various bias conditions which serve to enhance or suppress the different mechanisms.

Phase I of the program was devoted to studying a single transistor type under a variety of conditions for the purpose of identifying the mechanisms, establishing the models and understanding surface behavior under thermal, electrical or ionizing radiation stresses. Phase II involves the evaluation of a variety of transistors with different surface treatments, construction techniques and manufacturing processes. Results of this evaluation coupled with Phase I results will lead to recommendations for screening techniques and for device construction to minimize surface radiation effects.

## SECTION 1

### INTRODUCTION AND SUMMARY

A Phase I vacuum-irradiation test and six Phase II tests were performed during the fourth quarter. The effects of bias-radiation stresses on transistors in vacuum were compared with the effects for identical stresses in the normal nitrogen ambient. Little difference was detected in unbiased and forward biased transistors irradiated in both dry nitrogen and vacuum. In nitrogen, reverse collector-base bias caused extensive channeling in both junctions, with consequent large  $h_{FE}$  and  $I_{CBO}$  degradation. Devices irradiated in a vacuum with collector-base reverse bias exhibited considerably less  $h_{FE}$  and  $I_{CBO}$  degradation. The improvement in vacuum occurred early in the irradiation period where channeling is dominant in n-p-n devices, which indicates that evacuation results in a reduction of the channel component. Damage characteristics after large doses where surface space charge region recombination-generation was dominant, tended toward independence of either nitrogen or vacuum.

Analysis of Phase II tests indicated that  $h_{FE}$  is more vulnerable to channeling in p-n-p devices than in n-p-n's, since the channel in p-n-p devices is retained after large doses (unlike n-p-n's). While  $h_{FE}$  damage buildup after large doses was large in p-n-p devices compared with n-p-n's,  $I_{CBO}$  was not significantly higher in either p-n-p's or n-p-n's.

*Author*

## SECTION 2

### FOURTH QUARTER TESTS

The vacuum test initiated in the last quarter was completed during this period, thereby concluding the Phase I tasks of the contract. Fourteen tests are scheduled to fulfill Phase II of the contract, six of which were accomplished during the fourth quarter.

#### 2.1 PHASE I, TEST 11--VACUUM TEST

The purpose of this test was to investigate the surface damage buildup characteristics of oxide passivated planar transistors subjected to various bias-radiation stresses in a vacuum. Ionization of the gas ambient in which transistors are fabricated, and the subsequent deposition of positive charge on the oxide surface of planar transistors is held accountable for the inversion of p material beneath the oxide and the eventual channeling of the emitter-base and collector-base junctions. A decrease in channeling and hence a lessening of  $h_{FE}$  and  $I_{CBO}$  damage buildup in transistors was expected as a result of removing the gas ambient (by enclosing the transistors in evacuated envelopes) and subjecting these devices to the same bias-radiation stresses that were applied in the nitrogen ambient.

A pilot test was performed on a single 2N1613 transistor by removing the top of the can and mounting the transistor in a Kovar and glass envelope, shown in Figure 1, which was then evacuated to about  $10^{-10}$  Torr at  $25^{\circ}\text{C}$ . Three bias-radiation stress periods were alternated with high-temperature recovery periods. A bias of  $V_{CB} = +12\text{ V}$  was used during the first two bias-radiation periods, and the device was irradiated passively during the third radiation stress period.  $\frac{1}{h_{FE}}$  vs dose characteristics appeared very similar for all three test cycles despite the passive irradiation during the third cycle.

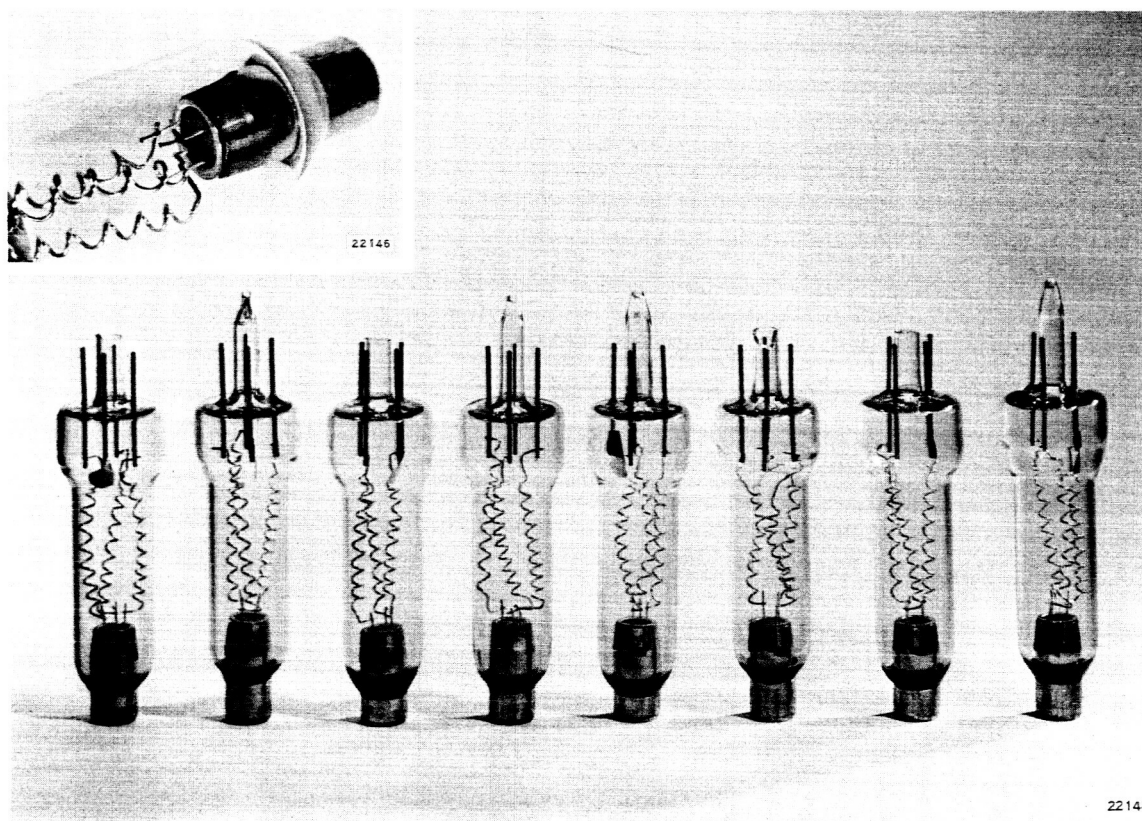


Figure 1 - Ultrahigh Vacuum Envelopes for Irradiating Transistors

Since no problems were encountered during the pilot investigation, eight additional 2N1613 transistors were sealed in envelopes at a vacuum on the order of  $2$  to  $3 \times 10^{-8}$  Torr. Table 1 summarizes the biases during irradiation for the test. Four of the vacuum envelopes were opened after the first three cycles, and two additional test cycles were performed (with half of the devices in air and the other half in vacuum).



Table 1 - Vacuum-Irradiation Test for Phase I

Device No.	Bias Conditions During Irradiation				
	Cycle 1	Cycle 2	Cycle 3	Cycle 4	Cycle 5
10	Passive	$V_{EB} = +3V$	$V_{CB} = +6V$	$V_{CB} = +6V^*$	Passive*
25	Passive	$V_{EB} = +3V$	$V_{CB} = +6V$	Passive	Passive
36	Passive	$V_{CB} = +12V$	$V_{CB} = +50V$	$V_{CB} = +12V^*$	Passive*
40	Passive	$V_{CB} = +12V$	$V_{CB} = +50V$	Passive	Passive
30	Passive	$I_C = 8mA, I_B = 2mA$	$I_B = 10mA, I_C = 0$	$I_B = 10mA, I_C = 0^*$	Passive*
33	Passive	$I_C = 8mA, I_B = 2mA$	$I_B = 10mA, I_C = 0$	Passive	Passive
7	Passive	$V_{CB} = +6V, I_C = 10mA$	$I_B = 10mA, I_C = 0$	$V_{CB} = +6V, I_C = 10mA^*$	Passive*
29	Passive	$V_{CB} = +6V, I_C = 10mA$	$I_B = 10mA, I_C = 0$	Passive	Passive

P-4078

\* This device was in air ambient during this test cycle

The expected extreme changes in damage buildup did not materialize, since channels still occurred in the evacuated devices subjected to bias-radiation stresses. Damage buildup in passive and forward biased devices in vacuum was similar to that in nitrogen ambient.

The most prominent result, however, was that vacuum appeared to inhibit damage buildup in devices irradiated with reverse biased junctions. Transistors having active biases, and  $V_{CBO} = 12V$ ,  $V_{CBO} = 6V$  and  $V_{EBO} = 3V$ , exhibited smaller collector-base and emitter-base channels, which significantly reduced the damage buildup rate early in the irradiation periods (low radiation doses). After large doses, induced  $h_{FE}$  and  $I_{CBO}$  damage buildup characteristics were independent of the nitrogen and vacuum ambient. The plots of the two transistors in Figure 2 demonstrate these characteristics. Device 35 was selected for illustrative purposes because of its relatively good tolerance to radiation, and Device 40 because of its considerable sensitivity. Although damage is still induced in both devices, the

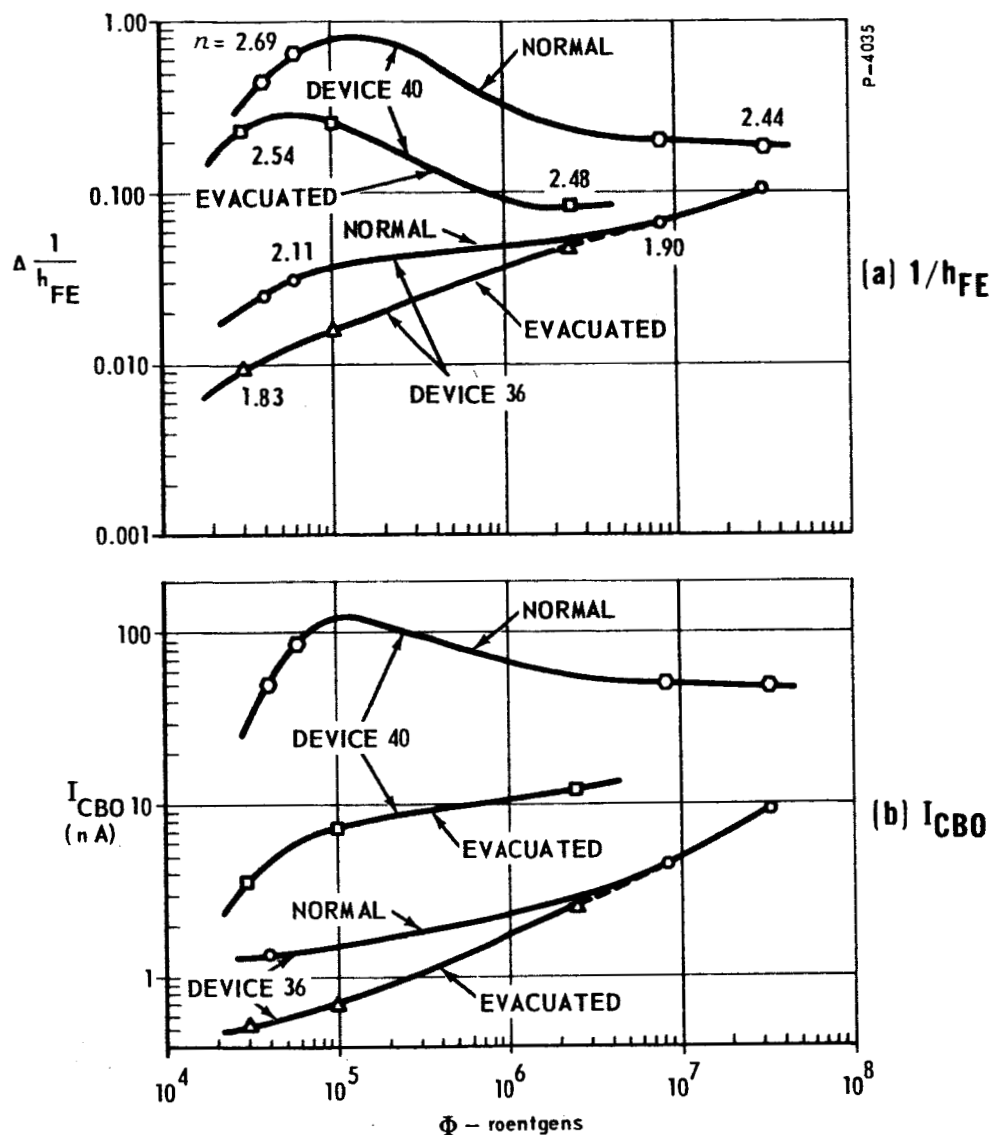


Figure 2 -  $1/h_{FE}$  and  $I_{CBO}$  Versus Dose for Normal and Evacuated Ambients on Devices 36 and 40

reduction of  $h_{FE}$  and  $I_{CBO}$  damage buildup rate is clearly evident at low doses. The independence of the damage to the ambient at large doses may also be observed in the figure.

Other observations, not well understood at this time, require additional analysis. A discrepancy was observed in slope constants  $n$  and channel capacitances in passively irradiated transistors. Those transistors that were stressed in air following stresses with the same reverse bias conditions used in nitrogen and vacuum ambients provided results that require further study. Damage induced in air, although greater than that induced in vacuum, was considerably less than that induced in nitrogen, indicating that the prior vacuum irradiation was effective in reducing some contribution to the damage.

## 2.2 PHASE II TESTS

Six Phase II tests were accomplished using the same general test procedure described in Section 4 of the Third Quarterly Report. The collector-base junctions of all test devices were reverse biased at 12 V and irradiated at  $\dot{\phi} = 1.67 \times 10^5$  R/hr until channel formation became evident, usually by means of capacitance measurements. Sometimes capacitance changes were too small to detect by measurement even though channels were formed. In those cases, irradiation was continued for 30 to 45 minutes and data were recorded to provide an early data point. The irradiation rate was then increased to  $\dot{\phi} = 5 \times 10^5$  R/hr until the rate of damage buildup was very small (after about 10 to 16 hours). The tests consisted of two periods of identical bias-radiation stresses separated by a high temperature recovery period.  $h_{FE}$ ,  $I_{CBO}$ ,  $C_{CB}$ ,  $C_{EB}$ , and reverse junction V-I data were recorded during each radiation stress period as follows: prior to irradiation, after channels had been induced (or at an early irradiation point), and after a large dose ( $\phi > 5 \times 10^6$  R). Table 2 summarizes the devices tested in the six tests.

The preliminary analysis consisted of plotting  $\frac{1}{h_{FE}}$ ,  $I_{CBO}$  and junction capacitance vs dose for each test cycle to indicate the spread among the test devices at each data point and the repeatability of

Table 2 - Phase II Tests

Test	Subject Transistor	Mfr.	Device Type
II-1	2N1613	FSD	High frequency, n-p-n
II-2	2N2222	Mota	High frequency, n-p-n, with annular ring
II-3	2N2219A	Mota	High frequency, n-p-n, some modified with metallization over emitter-base junction
II-4	2N2905	Mota	High frequency, p-n-p
II-5	2N2222	FSD	High frequency, n-p-n, without annular ring
II-6	2N1132	TI	High frequency, p-n-p, with field plate

P-4078

device surface damage. Those devices with damage behavior significantly greater or less than the others were easily identified. As an example of the data obtained, Figure 3 shows  $\frac{1}{h_{FE}}$  and  $I_{CBO}$  vs dose plots for seven of the 2N1613s tested in Test II-1 for two cycles. Transistor 40 stands out as an example of a device with poor surface characteristics since it develops considerably more  $I_{CBO}$  and  $h_{FE}$  damage than others. Note, however, that before both test cycles, initial  $h_{FE}$  and  $I_{CBO}$  values for Device 40 were not significantly different from others in the group.

Damage data for groups of devices indicate good repeatability of damage response with dose in sequential damage cycles followed by removal cycles. For any particular device, absolute repeatability may not be apparent because damage buildup is frequently less in the second test cycle than in the first, i.e., recovery often produces characteristics better than those of the original devices. Development of an analysis technique that would normalize damage may be desirable so that a more understandable and realistic comparison of the two test cycles can be made.

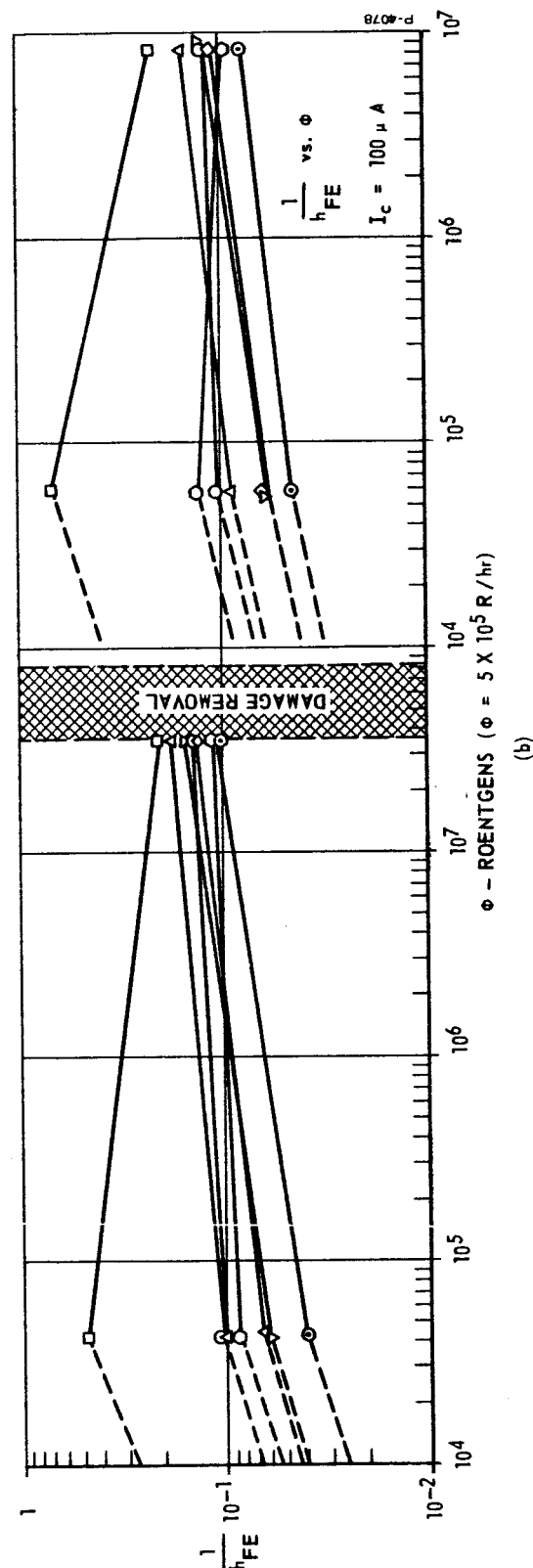
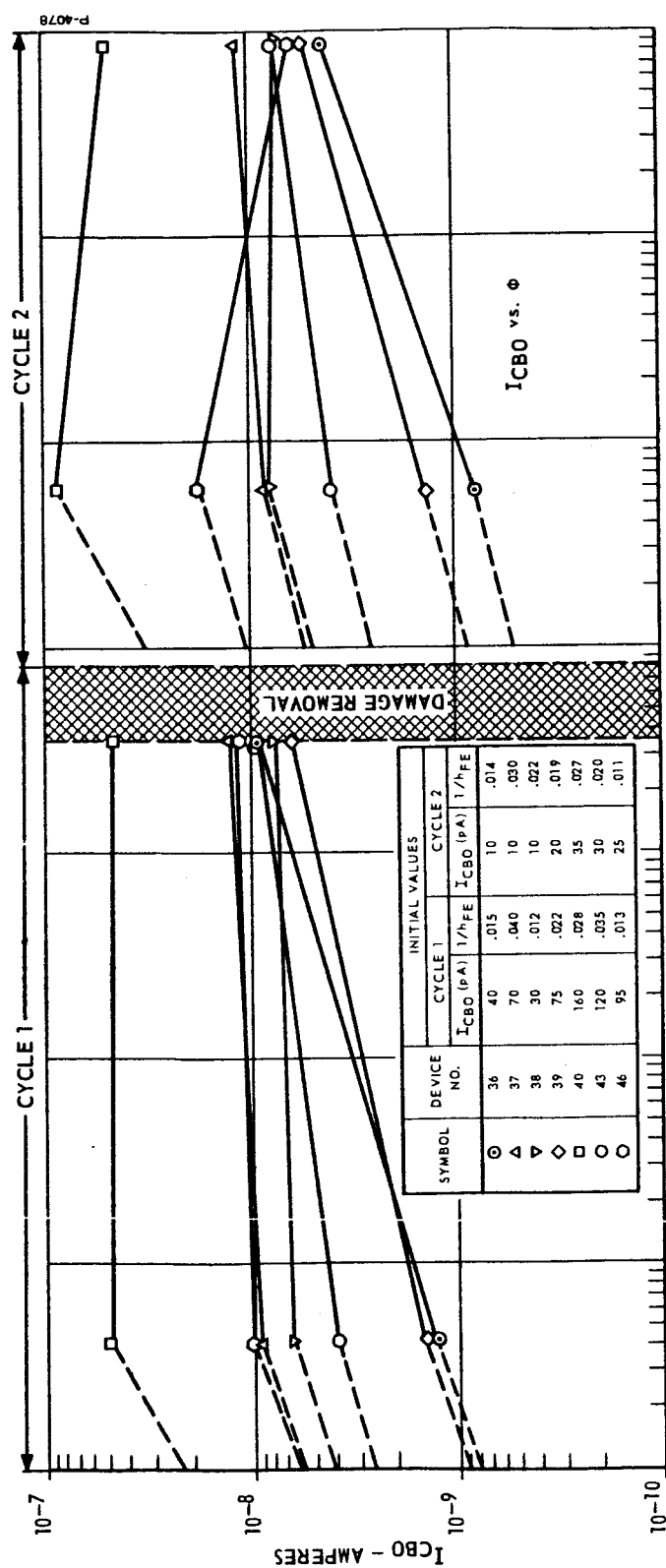


Figure 3 - 1/h<sub>FE</sub> and ICBO Versus Dose for Two Cycles of Test II-1

Slope constants,  $n$ , were also obtained and analyzed to provide an indication of the type of damage mechanism, e.g., low-dose channel component, high-dose recombination-generation component, etc. Table 3 is a listing of a representative sample of n-p-n and p-n-p transistor slope constants for low and high doses for each of two cycles. Values of  $n$  greater than 2 indicate a channel component of damage, while values near 2 generally indicate a recombination-generation component of damage.

Analysis of the Phase II tests shows that damage characteristics varied among the various device types subjected to the same bias-radiation stresses. The salient characteristic differences immediately categorized transistors into two groups: n-p-n and p-n-p. All of the n-p-n devices tested in this program reacted to reverse bias (12 V collector-base junction bias)-radiation stress by developing channels at low doses, which receded as the dose increased. Contrarily, p-n-p devices, although designed with metallic field plates, semiconductor guard rings, etc., in attempts to inhibit channeling, developed channels early in radiation which became increasingly large as radiation increased. These conclusions are supported by the slope constant data in Table 3.

The observation that channeling did not decrease at large doses in p-n-p transistors is explained by the damage model proposed in the Second and Third Quarterly reports. In n-p-n devices, photoemission of electrons from the channel in the p base region into the oxide layer resulted in a channel recession. For the p-n-p device, however, photoemission apparently did not take place and the channels increased with increased radiation. A more complete discussion of this mechanism will be presented in the final report. Additional discussion on the subject is also presented in the section on Model Discussion in Appendix A.

Capacitance data appear to substantiate the difference in channel growth and recession between n-p-n and p-n-p transistors. For n-p-n transistors,  $C_{CB}$  increases and reaches a maximum at low dose levels ( $\phi \leq 10^5$  R), after which it decreases to near its original value. Buildup of  $C_{EB}$  usually lags that of  $C_{CB}$ , and changes are not nearly as

Table 3. Slope Constants for n-p-n and p-n-p  
Devices as a Function of Dose

		A		B		
		Cycle 1		Cycle 2		
Transistor		<i>n</i>	<i>n</i>	<i>n</i>	<i>n</i>	
		Small Dose	Large Dose	Small Dose	Large Dose	
2N2219A	1*	2.06	1.9	2.07	1.93	n-p-n
Mota	2*	2.1	1.86	2.18	1.91	
	4*	1.99	1.94	1.97	1.88	
	6*	2.01	1.86	2.13	1.91	
	7	5.14	1.97	4.51	2.37	
	8	3.54	2.34	2.10	1.94	
	10	2.48	2.22	2.72	1.92	
2N2222	3	2.71	1.96	2.31	1.94	
Mota	4	2.89	1.99	3.12	2.01	
	7	2.13	1.97	2.18	1.98	
	9	2.98	1.99	3.42	1.98	
2N2222	13	2.38	2.02	3.17	2.06	
FSD	18	2.65	1.93	2.83	1.97	
	22	2.3	1.97	2.62	2.0	
	23	1.99	1.97	2.01	1.97	
2N1613	39	2.0	1.95	2.16	1.96	p-n-p
FSD	43	2.33	2.12	2.26	2.01	
	46	2.6	2.02	3.43	1.98	
	47	2.19	2.02	2.35	2.07	
2N1132	2	2.3	2.44	2.1	2.42	
TI	3	1.98	2.27	1.74	2.13	
	7	2.08	2.17	2.34	2.35	
	8	2.02	2.41	2.28	2.42	
	10	1.9	2.34	2.08	2.27	
2N2905	1	2.26	2.7	2.06	2.49	
Mota	2	2.14	2.55	2.06	2.45	
	3	2.31	2.78	2.07	2.61	
	4	2.08	2.59	1.97	2.51	
	5	2.21	2.6	2.04	2.54	

\*This is a specially prepared device with metallization over the emitter-base junction.

large as those of  $C_{CB}$ .  $C_{EB}$  also tends to reach a maximum after which it decreases to near normal as shown in Figure 4b. For p-n-p devices, changes in  $C_{CB}$  are similar to those observed for n-p-n; however,  $C_{EB}$  remains constant or slightly increases in the p-n-p devices, indicating a possible continuation of channel growth. The reason the increasing emitter-base channel is not clearly reflected in  $C_{EB}$  changes in p-n-p devices is because the instrumentation resolution is not adequate to permit detection of small capacitance changes. It appears, therefore, that while changes in capacitance were an effective tool for monitoring channel buildup and decay in some devices, (particularly the Fairchild 2N1613 which displayed  $C_{CB}$  increases as high as 600 percent and  $C_{EB}$  increases as high as 400 percent), device geometry and channel characteristics of other devices tend to preclude the exclusive use of capacitance to detect channels because of relatively small capacitance changes and limitations in the resolution of the instrumentation.

Generally, considering their shapes, plots of junction capacitance and slope constant  $n$  versus  $\phi$  (Figure 4), can be correlated with increases and decreases in  $n$ . Magnitudes of  $n$ , junction capacitance and  $h_{FE}$  degradation apparently do not correlate closely due primarily to differences in sensitivities of various devices to the same stress.

In n-p-n devices collector-base junction breakdown voltage tends to decrease with increases in dose, while the emitter-base junction breakdown voltage remains essentially constant. For the p-n-p devices tested, the data are not quite so revealing and no positive statements can be made concerning changes in breakdown voltage as a function of dose.

Motorola 2N2219A n-p-n transistors with metallization over the emitter-base junction were compared with ordinary devices of the same type. Preliminary analysis of the slope constants (Table 3) indicated that the metallization was effective in reducing emitter-base channel formation. For the special devices, values of  $n$  were near 2 at low doses and less than 2 after large doses, as compared with  $n$  values as



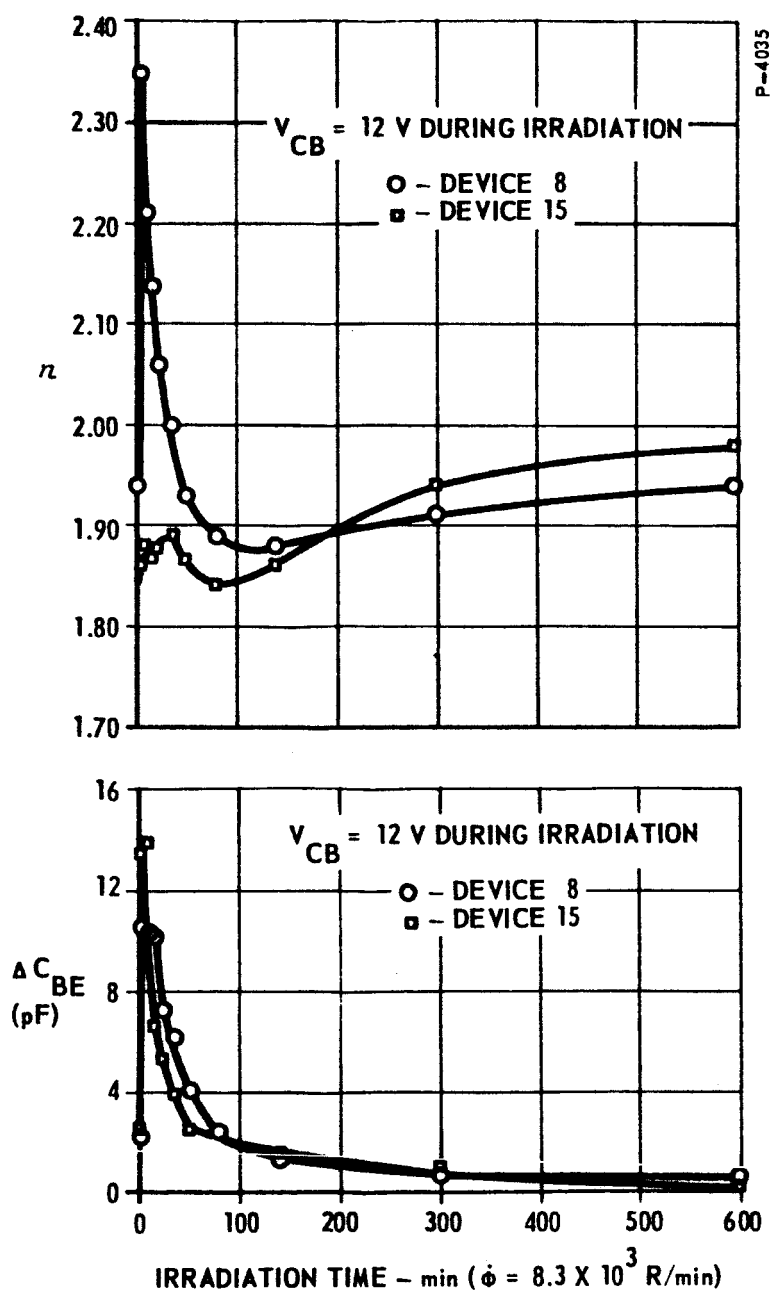


Figure 4 - Exponential Slope Constant and Base Emitter Capacity as a Function of Irradiation Time - Devices 8 and 15

high as 5 at low doses and greater than 2 after large doses for most of the standard devices. Changes in  $C_{EB}$  were too small to measure with the instrumentation available, so convincing corroborating evidence could not be provided. The surprising fact however, is that  $h_{FE}$  and  $I_{CBO}$  degradations were not significantly different between the two groups of transistors, even though large differences were observed in channel formation. Also, the data for the special devices were much more consistent and uniform, while the data for the standard devices were more random with a wider spread. Additional analyses of the data are required before final conclusions on the effects of metallization can be made.

### SECTION 3

#### FURTHER ACTION REQUIRED

Attempts will be made to determine the causes of decreased damage buildup characteristics in those devices irradiated in air after irradiation in vacuum.

Further analyses will be made to correlate noticeable differences in the damage buildup characteristics of both test cycles to verify repeatability of device susceptibility to surface degradation, and hence prove the validity of the X-ray irradiation-high temperature recovery transistor screening cycle.

Analysis will lead to identification of those devices that have the greatest immunity to surface degradation and those device types tested that most readily lend themselves to the above mentioned screening technique.

Additional data reduction and analysis will be performed to resolve the apparent conflict regarding the effect of metallization. Slope constants indicate that metallization greatly reduces channel formation; yet the changes observed in  $h_{FE}$  and  $I_{CBO}$  are minor.

APPENDIX A to Bendix RLD Report 3557

PREPRINT

MECHANISMS OF IONIZING RADIATION  
SURFACE EFFECTS ON TRANSISTORS\*

By

David L. Nelson and Richard J. Sweet

The Bendix Corporation  
Research Laboratories Division  
Southfield, Michigan

July 11, 1966

IEEE Annual Conference on  
Nuclear and Space Radiation Effects  
Palo Alto, California  
July 18-22, 1966

\* Work done under Contract NAS 8-20135

## INTRODUCTION

Surface effects on silicon planar bipolar and MOS transistors induced by ionizing radiation have been studied by several investigators, using as radiation sources Co-60 gamma,<sup>1-3</sup> electrons,<sup>4-6</sup> X-rays,<sup>7-9</sup> gas ion bombardment,<sup>10</sup> and even space radiation via orbital tests.<sup>1</sup> The first model to explain leakage current and gain changes in bipolar transistors was proposed by Peck et al<sup>11</sup> based on studies of exposure to ionizing radiation of silicon mesa transistors which were not SiO<sub>2</sub> passivated.  $h_{FE}$  and  $I_{CBO}$  degradation, according to this model, are due to surface channels produced by an accumulation of charged ambient gas ions on the device surface. These gas ions are attracted to the transistor surfaces by electric fields produced when the device is electrically biased. A more recent investigation<sup>10</sup> modifies this model for SiO<sub>2</sub> passivated devices, suggesting that actual deposition of gas ions on the oxide surface does not occur, but that instead ions traveling very close to the surface give up their charge to oxide surface "sites."

Several investigations<sup>5,6,7,9</sup> of ionizing radiation effects on MOS structures have shown the existence of a second mechanism for surface degradation--migration of charged species in the SiO<sub>2</sub> insulating layer when an electric field is applied across the oxide layer. Either of these mechanisms results in an accumulation of space charge over silicon, altering the surface potential of the semiconductor. This change in silicon surface properties is usually reflected by enhancement, depletion or inversion of surfaces, changes in surface recombination velocity, and changes in p-n junction characteristics.

Investigators hold opposing views as to which of the above mechanisms dominates for silicon planar bipolar transistors. Hughes<sup>2</sup> concludes, from Co-60 irradiations of normal and evacuated 2N2801 p-n-p transistors that ionizing radiation surface effects occur as a result of drift of mobile space charge in the SiO<sub>2</sub> layer and not as a result of conditions external to the wafer. Stanley<sup>4</sup> concurs with this conclusion. Hogrefe<sup>1</sup> reports that normal 2N1711 n-p-n planar transistors irradiated in the Van Allen belts suffered considerable loss of gain, while devices evacuated by piercing the encapsulating can suffered almost no gain loss after 100 days in orbit ( $\sim 10^5$ R). He concludes that gas ionization is the cause of these surface effects.

The intent of the investigation described in this paper is to study in detail the ionizing radiation effects produced by X-rays as a radiation source on silicon planar bipolar transistors to determine dominant degradation mechanisms and the conditions under which each mechanism dominates. The effects of various electrical bias conditions during irradiation on  $h_{FE}$  and  $I_{CBO}$  degradation were measured to determine the relative amounts of degradation over a wide range of measurement conditions. To study the importance of gas ionization, an ultrahigh vacuum ( $\sim 10^{-8}$ Torr) test was performed. Also investigated were temperature annealing of damage and the time and dose dependence of damage buildup.

$h_{FE}$  degradation was caused by base region recombinations near the surface at high measuring currents and channel current  $I_{CH}$ , and by surface space charge region recombination-generation current  $I_{SRG}$  at low

measuring currents. The latter two currents were also responsible for  $I_{CBO}$  increases. The relative and absolute magnitudes of  $I_{SRG}$  and  $I_{CH}$  vary with measurement conditions, bias during irradiation, and dose. The resultant magnitude and rate of damage buildup was very dependent on these conditions. A radiation screening cycle was developed, in which temperature annealing is used to remove all the X-ray induced damage, thus enabling identification of device sensitivities to radiation. Temperature annealing enabled series (or sequential) testing, by which a single device can be tested under several different bias conditions by first irradiating at one condition, next annealing to remove the induced damage and then irradiating at a second condition.

A model is proposed to describe the mechanisms of oxide space charge buildup over the silicon layer, which makes use of both charge deposition on the oxide surface and charge migration in the oxide. Charge migration in the  $SiO_2$  layer under the influence of junction fringing fields explains the accumulation of damage in devices irradiated with electrical bias conditions that do not create significant electric fields in the ambient gas surrounding the device. A more complex proposed model accounts for the damage accumulated when a device is irradiated with the bias condition, such as reverse biased collector-base junction, which produces an electric field in the surrounding ambient. This model, which differs for p-n-p and n-p-n devices, makes use of charge accumulation on the  $SiO_2$  surface due to ambient gas ions, charge migration in the oxide layer, and electron flow across the  $SiO_2$ -Si interface.

## EXPERIMENTAL PROCEDURES

Ionizing radiation exposures were accomplished using a 150 kvp X-ray machine with type 2N1613 (Fairchild) silicon planar n-p-n transistors as the major test vehicle. Cursory tests were also performed on several other devices including 2N2222 (Fairchild), 2N2219A (Motorola), 2N2222 (Motorola) which are n-p-n's and 2N1132 (Texas Inst ), 2N2905 (Motorola) and 2N3964 (Fairchild-Planar II) which are p-n-p's. X-rays of this energy are used since they produce ionizing radiation surface effects without the displacement type damage at large doses common to Co-60 gamma irradiation and high energy electron bombardment. Irradiation tests were performed at the maximum available rate of  $5 \times 10^5$  R/hr.  $I_{CBO}$ ,  $h_{FE}$ ,  $V_{BE}$ ,  $C_{BE}$  and  $C_{BC}$  were measured on test devices before, during and after irradiation at a temperature of  $35^\circ\text{C}$ , which was closely controlled by a thermoelectric element. All measurements were performed with the X-ray machine shut down to eliminate photocurrent effects and unstable surface effect components due to high X-ray rates that anneal out in several seconds.

### $h_{FE}$ Damage Component Identification

Current gain  $h_{FE}$  measurements were made with a collector-base voltage of 5.3 volts over a collector current range of  $0.1\mu\text{A}$  to  $10\text{mA}$ , using specially constructed instrumentation. Precise high-speed readings were possible with this system, because it minimized annealing of surface damage due to the measurement stress. High current ( $10\text{mA}$  to  $300\text{mA}$ )  $h_{FE}$  was measured at somewhat higher collector-base voltage due to collector resistance effects. These measurements were performed on a Birtcher Model 70 pulsed  $h_{FE}$  tester.



Reduction in  $h_{FE}$  due to ionizing radiation surface effects is caused by introduction of extra base current components which appear to shunt the base-emitter junction. Two base current components generated by ionizing radiation are surface space charge region recombination generation current  $I_{SRG}$  and surface channel current  $I_{CH}$ .<sup>12</sup>  $I_{SRG}$  is produced by recombination in the base-emitter space charge region of majority carriers from the base and emitter. This process takes place in the space charge region at the  $SiO_2$ -Si interface where a high concentration of energy states exists very close to the middle of the Si energy band. The resultant current component varies with base-emitter forward voltage as  $\exp \frac{q V_{BE}}{n k T}$  where  $(1 < n \leq 2)$ .<sup>12</sup> A more typical range for  $I_{SRG}$  is from 1.5 to 2.0.

Surface channels are formed when the oxide space charge above the silicon is of sufficient magnitude to cause inversion of the silicon under the  $SiO_2$ -Si interface. If p-material is inverted near a p-n junction, a channel is formed that appears as an extension of the n-side of the junction over the surface of the p-side. This increase in junction area results in an increase in junction capacitance and an increase in both forward (affects  $h_{FE}$ ) and reverse (affects  $I_{CBO}$ ) current. Capacitance changes are dependent on the extent of the channel; however, the magnitude of current component  $I_{CH}$  depends to a larger degree on the quality of the semiconductor surface at the  $SiO_2$ -Si interface. It has been demonstrated by Fitzgerald et al.<sup>13</sup> that large  $I_{CH}$  values are produced only when a combination of a channel and a poor semiconductor surface exists.

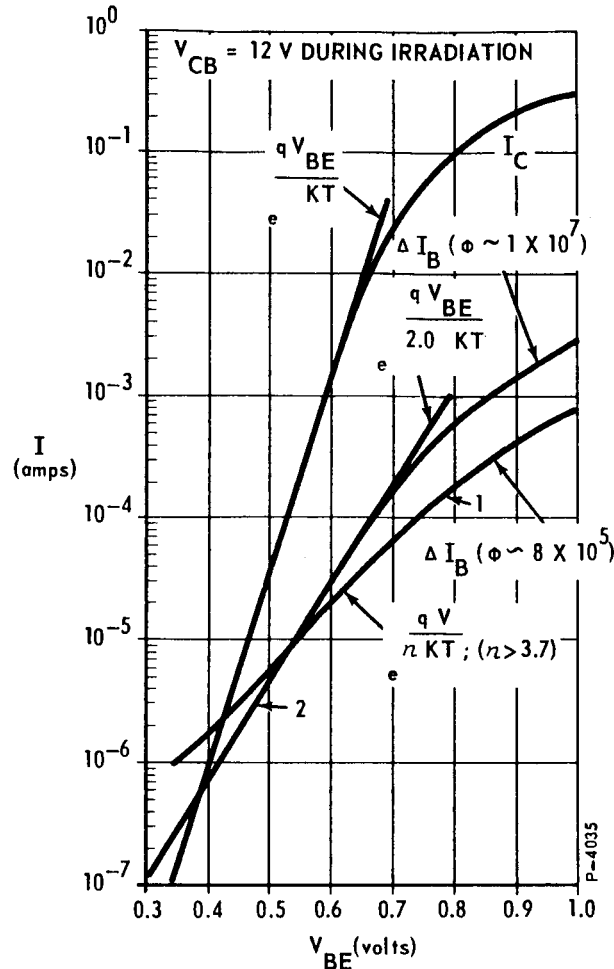


Figure 1 - Gain Degradation Produced by a Reverse Biased Collector-Base Junction During Irradiation

$I_{CH}$  components at the base-emitter junction also vary as  $\exp \frac{q V_{BE}}{n k T}$ . Like  $I_{SRG}$ , however, their exponential slope constant  $n$  is greater than 2. Figure 1 is a plot of collector current  $I_C$  and typical ionizing radiation induced excess base currents  $\Delta I_B$  versus  $V_{BE}$ . Curve 1 can be identified by its exponential behavior at low currents as an  $I_{CH}$  component, while curve 2 is an  $I_{SRG}$  component.  $1/h_{FE}$  is a convenient parameter to use when studying the effects of these components on  $h_{FE}$  since:

$$\frac{1}{h_{FE}} = \frac{I_{BO} + I_{SRG} + I_{CH}}{I_C} \quad (1)$$

where  $I_{B0}$  is the base current before surface damage. Subtracting initial  $1/h_{FE}$  from that measured after irradiation (defined as  $\Delta 1/h_{FE}$ ) provides a means of assessing the effect of excess base currents. Based on the exponential behavior discussed above for  $I_{SRG}$  and  $I_{CH}$  components, an expression for  $\Delta 1/h_{FE}$  is:

$$\Delta \frac{1}{h_{FE}} = \text{const} \times [I_C]^{\left(\frac{1}{n} - 1\right)} \quad (2)$$

where  $n$  is the exponential slope constant for the excess base current component. Figure 2 shows several plots of  $\Delta 1/h_{FE}$  vs  $I_C$  produced by X-ray radiation at various bias conditions during irradiation. The dashed line on this plot shows a typical initial  $1/h_{FE}$ . The linear portions of these curves at low collector currents are due to  $I_{SRG}$  components identified by  $n \leq 2$ . The hook-shaped region at high current depicts a damage component very similar in behavior to the normal base spreading resistance term in gain.

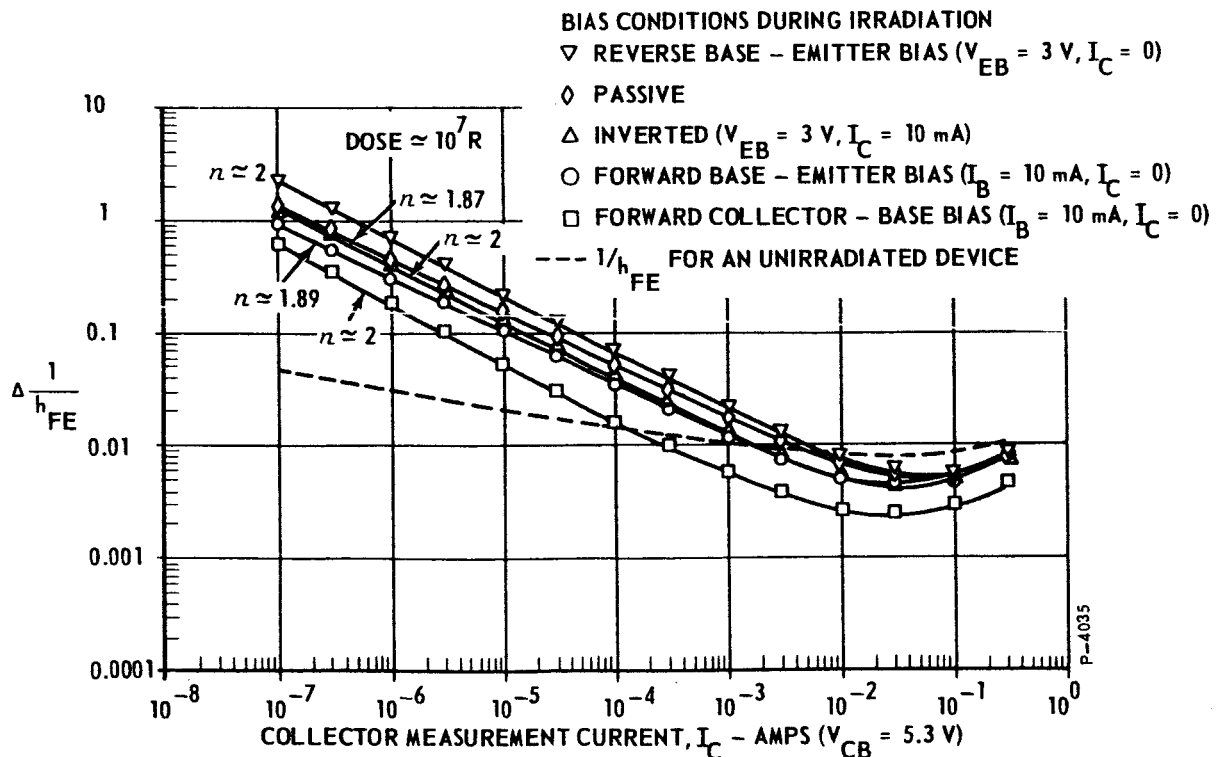


Figure 2 - Effect of Bias and Measurement Current on Current Gain Degradation

Determination of  $\beta$  at low measurement currents proved to be a very useful tool in identifying dominant damage mechanisms. All  $h_{FE}$  data were reduced by digital computer using a least square error fit to equation (2) at collector currents from 0.1 $\mu$ A to 1mA.

#### Series Test Procedure

A majority of the tests during this investigation were performed with a group of 15 devices, using a series test procedure. This procedure consisted of irradiating up to 12 devices at a time, followed by a 300°C, five-hour annealing cycle which returned the device parameters to a condition as good as or slightly better than their pre-irradiation measurements. Irradiating with the same conditions several times showed good repeatability, indicating that the temperature anneal provides complete recovery to initial conditions. Figure 3 shows the effectiveness of temperature stresses in removing  $h_{FE}$  degradation induced by ionizing radiation for 2N1613 transistors irradiated with a reverse collector-base bias, no bias, and an active bias.\*

---

\* The term "active bias" is used several times in this paper to denote the normal amplifying mode where the collector base junction is reverse-biased and the emitter-base junction is forward-biased. "Passive" is also used to denote the "no bias" condition.

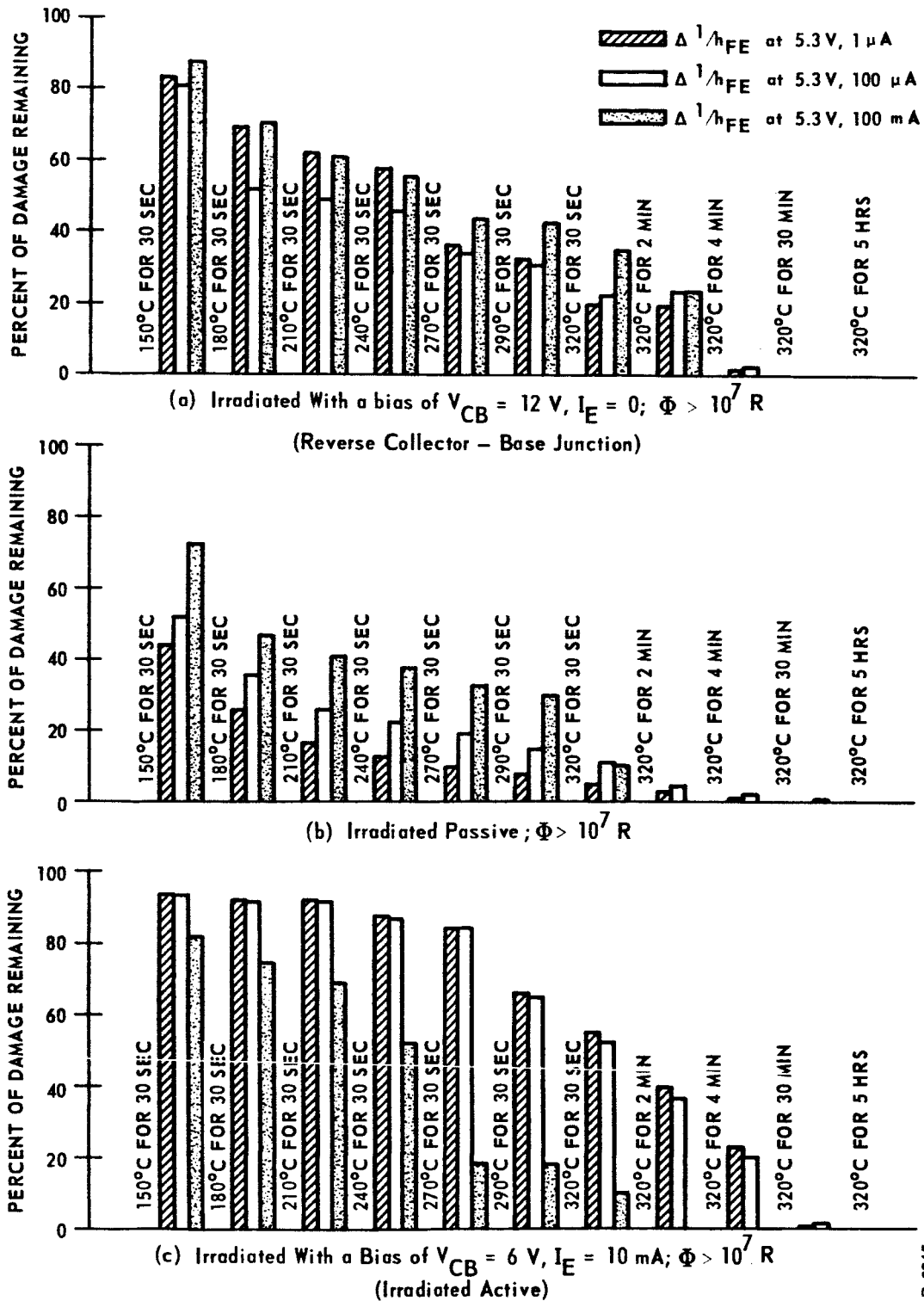


Figure 3 - Effect of Temperature Stress on  $h_{FE}$  Damage Removal

# EXPERIMENTAL RESULTS

Several X-ray irradiation tests were performed on 2N1613s to determine the rate and magnitude of damage buildup versus exposure time using the experimental procedures described above. Three silicon surface degradation mechanisms were produced by irradiation, including  $I_{SRG}$  and  $I_{CH}$ , which affect p-n junction characteristics causing changes in  $I_{CBO}$  and  $h_{FE}$  at low measurement currents, and a third mechanism which produces  $h_{FE}$  degradation at high measurement currents.

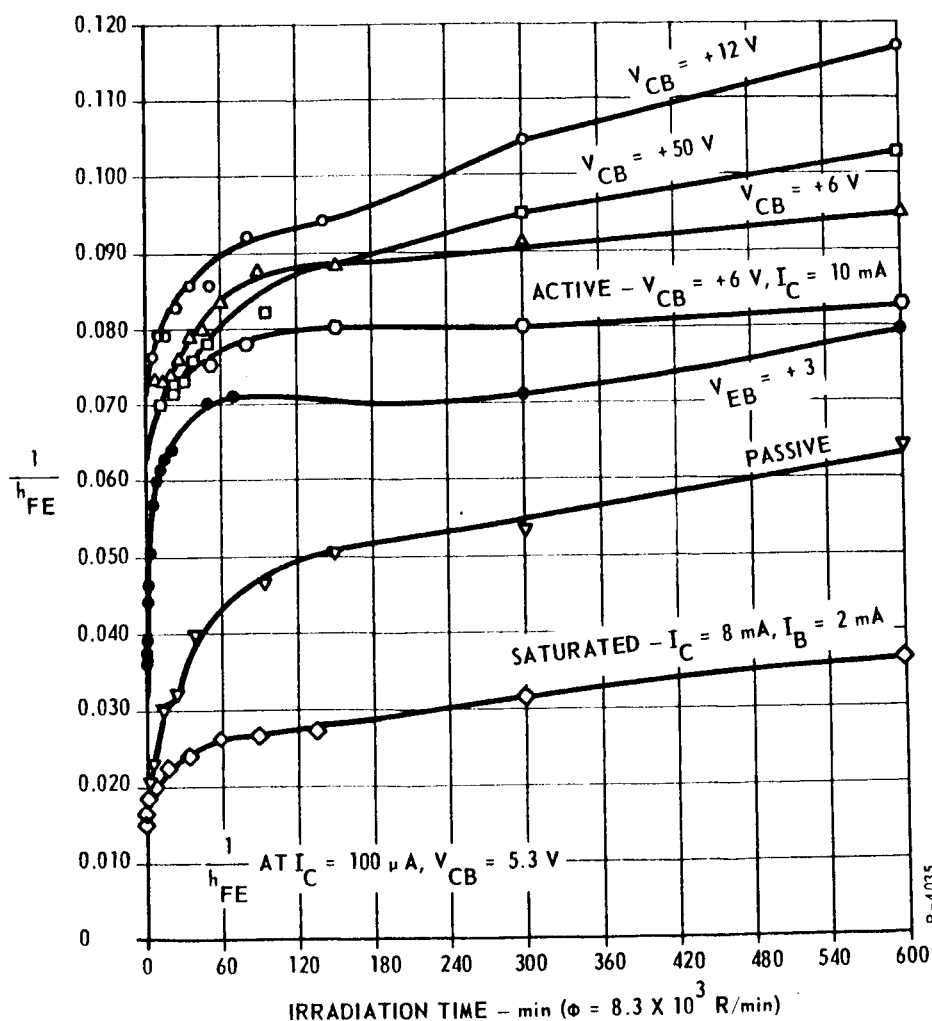


Figure 4 - Effects of Bias During Irradiation on Low Current  $h_{FE}$  Damage Buildup - Device 8

### Effects of Bias During Irradiation

The magnitude and rate of buildup of low current  $h_{FE}$  damage mechanisms proved to be strongly dependent on the electrical bias during irradiation. Figure 4 is a plot of  $1/h_{FE}$  ( $I_C = 100\mu A$ ) for a series test of several bias conditions during irradiation on a single 2N1613 using the series test procedure and annealing cycle described above. Gain degradation was smallest for a saturated device where both junctions were forward-biased during irradiation, while the most damage was produced when the collector base junction was reverse-biased and the emitter lead was open during irradiation. This strong dependence of  $h_{FE}$ , a base-emitter junction property, on collector base reverse bias suggests that conditions external to the silicon wafer are important in a damage model. For example, the saturated and active runs indicate that even though the base emitter junction was forward-biased at 10mA for both conditions, the active run with the reverse-biased collector base junction accumulated three or more times the damage incurred by the saturated run. A reverse bias on either junction during irradiation produced an initial rapid rise in gain damage which tended to saturate at large doses, while no bias or a forward bias produced a gradually rising damage component which also had a saturating tendency. The ultimate magnitude of gain damage at large doses for transistors with reverse-biased collector base junctions was greater than that sustained by transistors irradiated passively, with one exception. The ultimate damage for some devices irradiated actively (reverse-biased collector base junction and forward-biased base emitter junction) was less than that for passive

irradiation. In this case the collector base bias dominated early in the damage buildup period, producing a fast early rise in damage; while the base-emitter forward bias dominated at large doses, demonstrating the attenuating effect that a forward-biased base-emitter junction has on damage buildup.

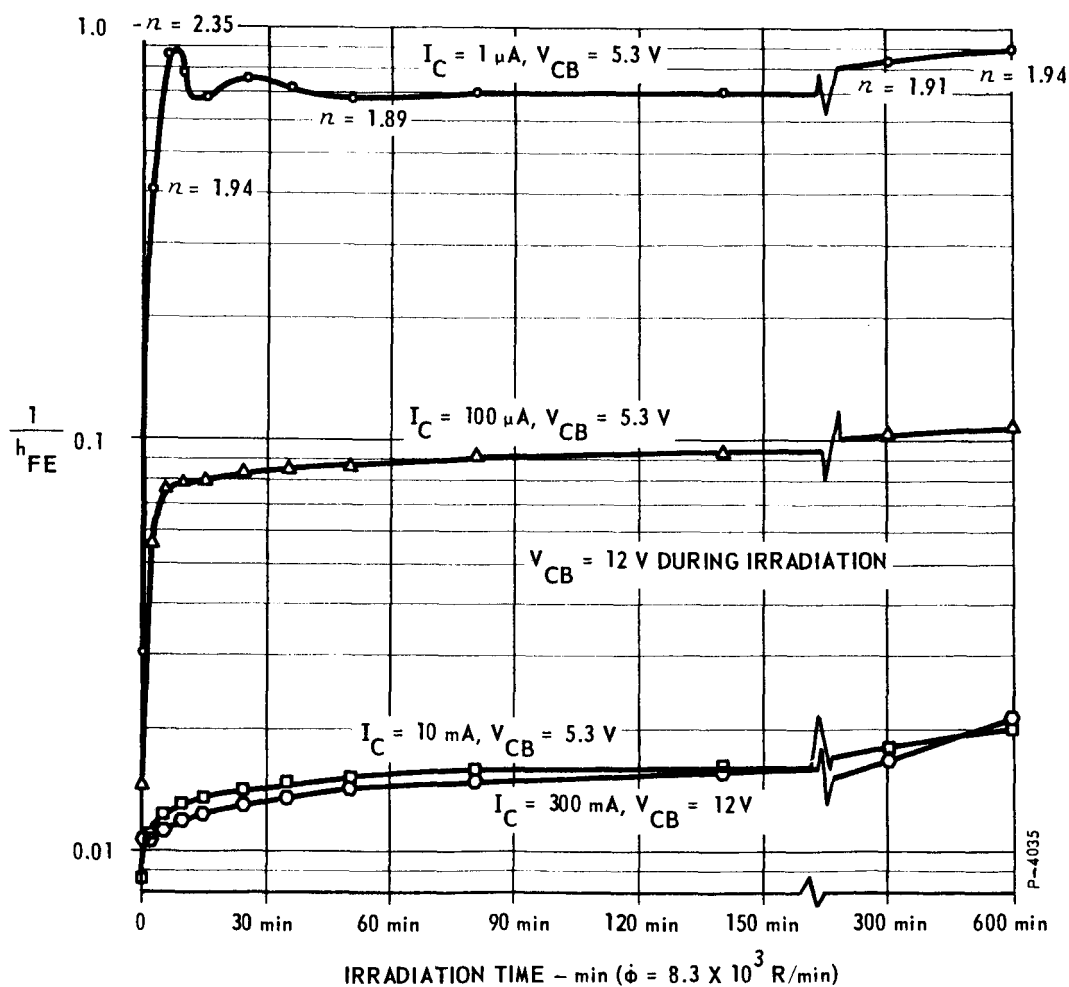


Figure 5 - Current Gain Versus Irradiation Time at Different Measuring Currents - Device 8



### Effect of Measurement Conditions

Figure 5 is a plot of  $1/h_{FE}$  measured at several collector currents versus exposure time for the 12-volt collector-base reverse-bias run of Figure 4. The rate and magnitude of damage buildup are much larger at low measuring currents than at high, with 300mA damage building up very gradually and  $1\mu A$  gain damage building up almost in a step function fashion, with a slight overshoot at very early doses. It is noteworthy that this rapid buildup of low current damage is accompanied by an  $n=2.35$ , indicating the existence of a channel current component; while the slope at the end of the run is 1.94, indicating an  $I_{SRG}$  damage component.

### Junction Capacitance Changes

Figures 6a, 6b, and 6c are plots of  $h_{FE}$  and  $I_{CBO}$  degradation along with junction capacitances versus irradiation time for passive, reverse collector-base junction, and active biases during irradiation. The passive run produced no significant changes in capacitances, indicating an absence of channels. Buildup of  $I_{CBO}$  and  $h_{FE}$  damage was gradual, and the  $n$  gradually increased from 1.71 early in the run to 1.92 at the end of the run, which is characteristic of  $I_{SRG}$  components. The active and reverse collector-base runs exhibited large changes in both  $C_{CB}$  and  $C_{BE}$  early in the run, accompanied by rapid  $h_{FE}$  damage buildup and  $I_{CBO}$  increases. A channel was apparently formed early in the irradiation, producing an  $n$  of 2.35 at its peak for the collector-base reverse bias run. At later exposures  $n$  decreased to less than 2,  $h_{FE}$  and  $I_{CBO}$  damage saturated, and  $C_{BE}$  and  $C_{BC}$  returned to their pre-irradiation values, indicating that the early channel had receded and that the dominant damage mechanism was  $I_{SRG}$ .

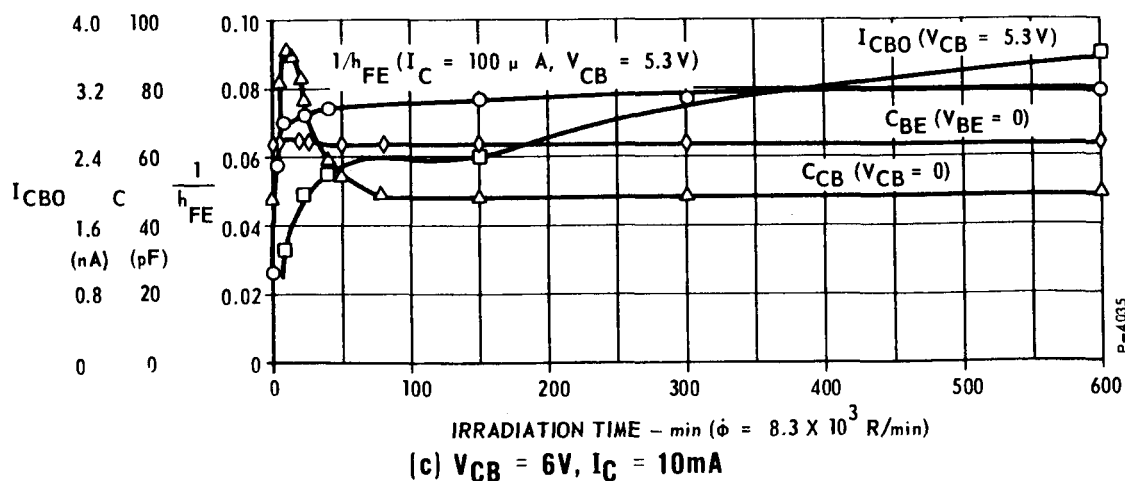
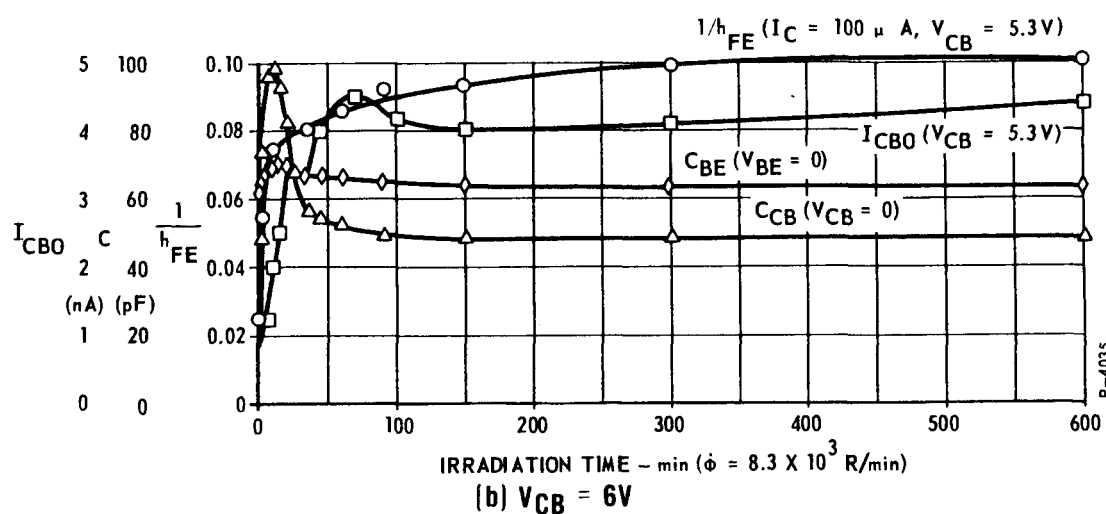
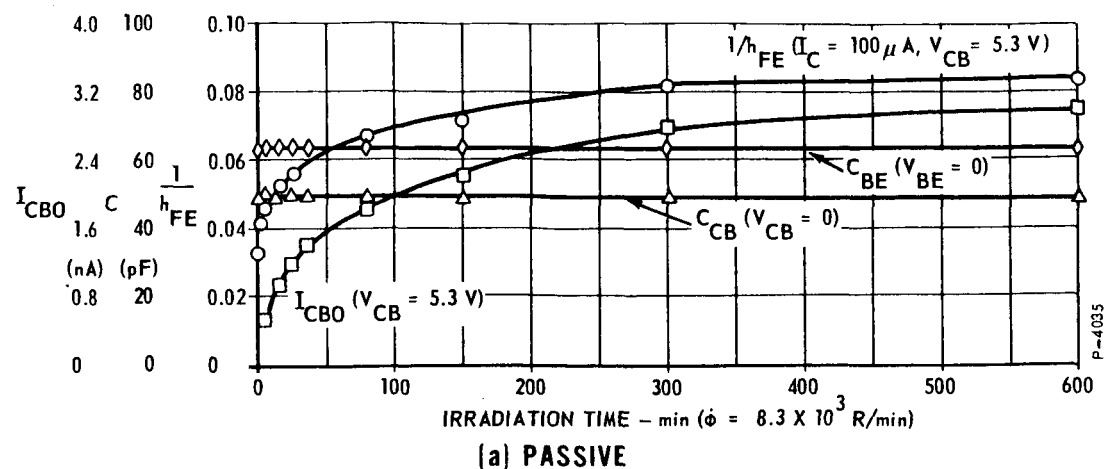


Figure 6 -  $1/h_{FE}$ ,  $I_{CBO}$  and Junction Capacitance as a Function of Exposure Time for Various Biases During Irradiation - Device 15

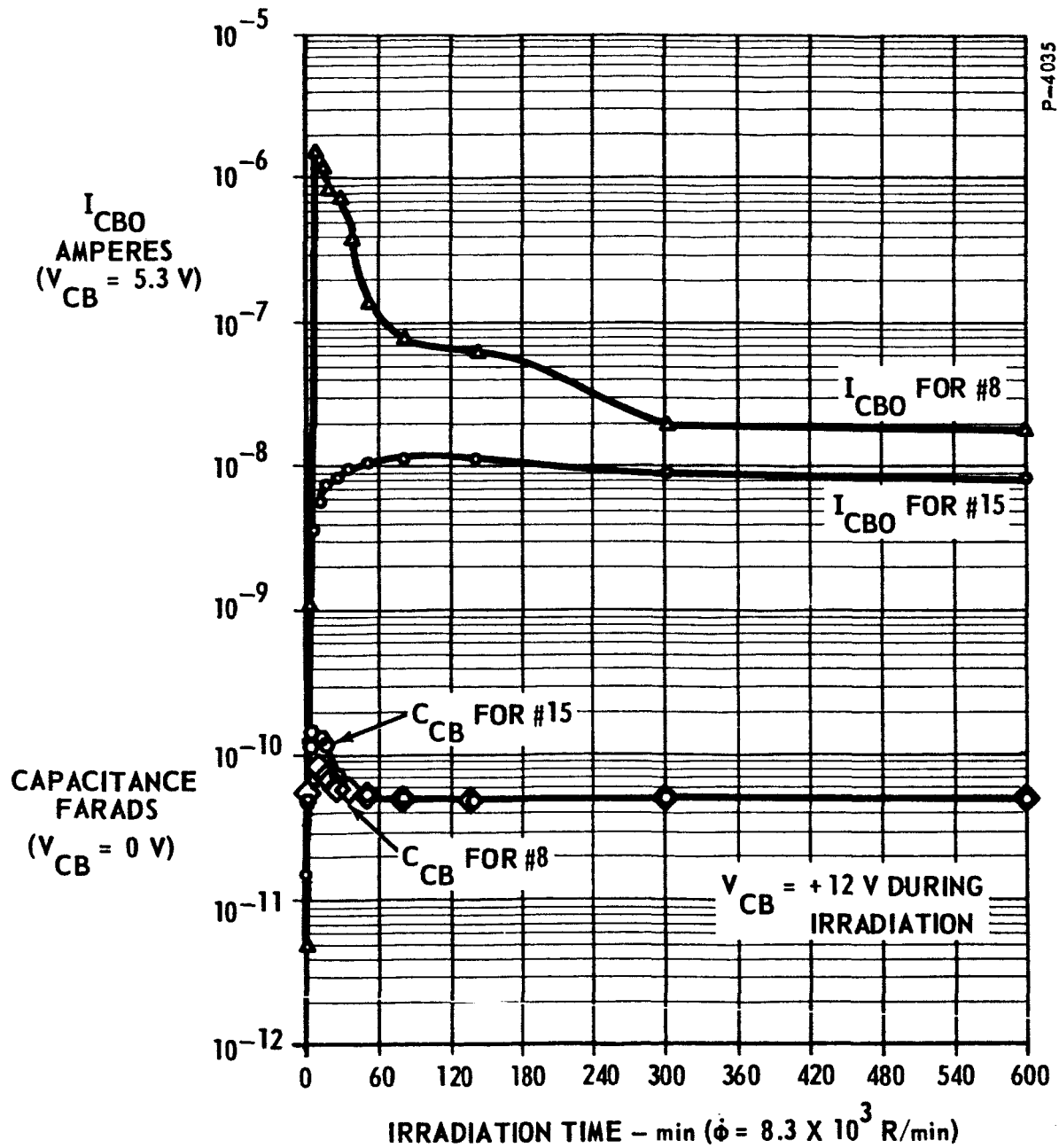
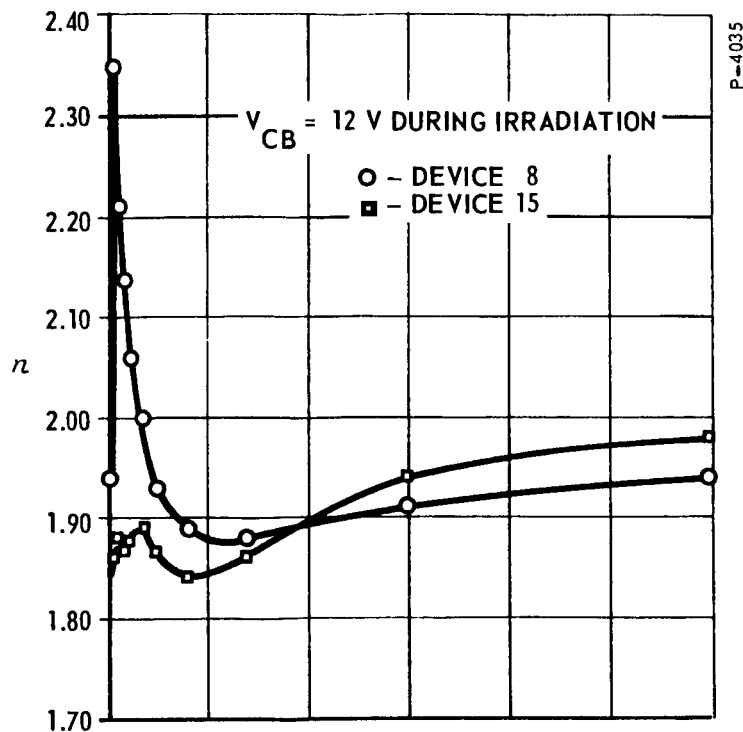
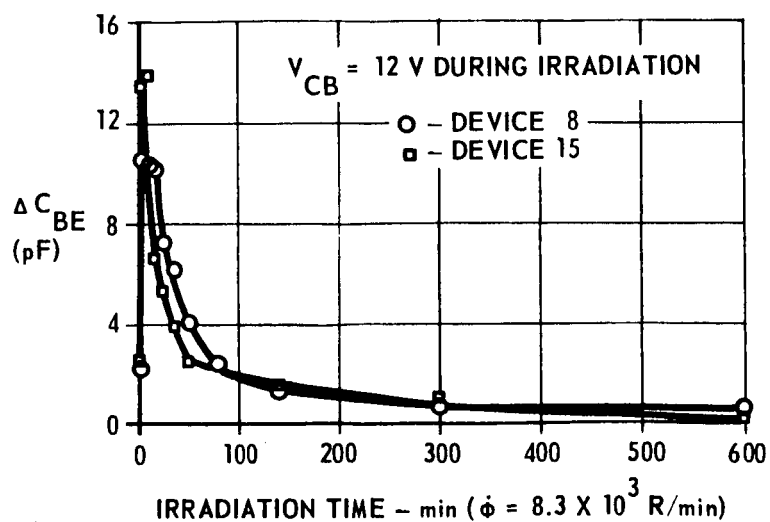


Figure 7 -  $I_{CBO}$  and  $C_{CB}$  Versus Irradiation Time - Devices 8 and 15



(a) EXPONENTIAL SLOPE  
CONSTANT



(b) CHANGE IN  $C_{BE}$

Figure 8 - Exponential Slope Constant and Base Emitter Capacity as a Function of Irradiation Time - Devices 8 and 15

Junction capacitance measurements provided an excellent means of monitoring the formation and decay of channels on 2N1613s. The magnitude of the capacitance measurement, however, was not indicative of the magnitude of  $I_{CBO}$  increases, gain damage or  $n$ , as is evident from Figures 7 and 8. Figure 7 shows  $I_{CBO}$  and  $C_{CB}$  as a function of exposure time for Devices 8 and 15. As can be seen, Device 15 which exhibited a larger change in junction capacitance, displayed an early leakage component two orders of magnitude less than Device 8.  $I_{CBO}$  variations similar to this have been reported by Peden et al.<sup>3</sup> Figure 8 is a similar plot showing the change in base emitter capacitance and  $n$  versus exposure time for the same two devices. Again, Device 15 exhibits a larger change in junction capacitance during the early buildup period. However, Device 8 exhibits the larger  $n$ , indicating that channel current is the dominant gain damage component in this device. This type of behavior enforces the theory of Fitzgerald and Grove<sup>13</sup> that channel current requires the simultaneous presence of a surface channel (inversion layer) and "generation sites."

#### Vacuum Test

It is difficult to explain the effect of collector-base reverse bias during irradiation on base-emitter properties without the gas mechanism originally proposed by Peck et al.<sup>11</sup> A test was designed to determine the effects of ultrahigh vacuum on the behavior of  $h_{FE}$  and  $I_{CBO}$  degradation. Eight type 2N1613 transistors with various radiation histories were individually evacuated in glass envelopes as shown in

Figure 9. The vacuum level achieved was about  $10^{-8}$  Torr. The same series test procedure discussed previously was followed to irradiate these devices with several electrical bias conditions during irradiation. No large difference in damage was observed between the normal nitrogen ambient and a vacuum, for devices with passive or forward biases during irradiation. This indicates that the component identified as  $I_{SRG}$  by  $n$  is independent of the ambient external to the wafer. Channeling during the early buildup was not eliminated by evacuation, but it was considerably reduced from the magnitudes encountered in the normal nitrogen ambient. For all reverse bias conditions investigated (active,  $V_{CB} = 12$  volts,  $V_{CB} = 6$  volts, and  $V_{EB} = 3$  volts) channeling tendency during early buildup and also changes in junction capacitance were less in vacuum than the normal nitrogen ambient.

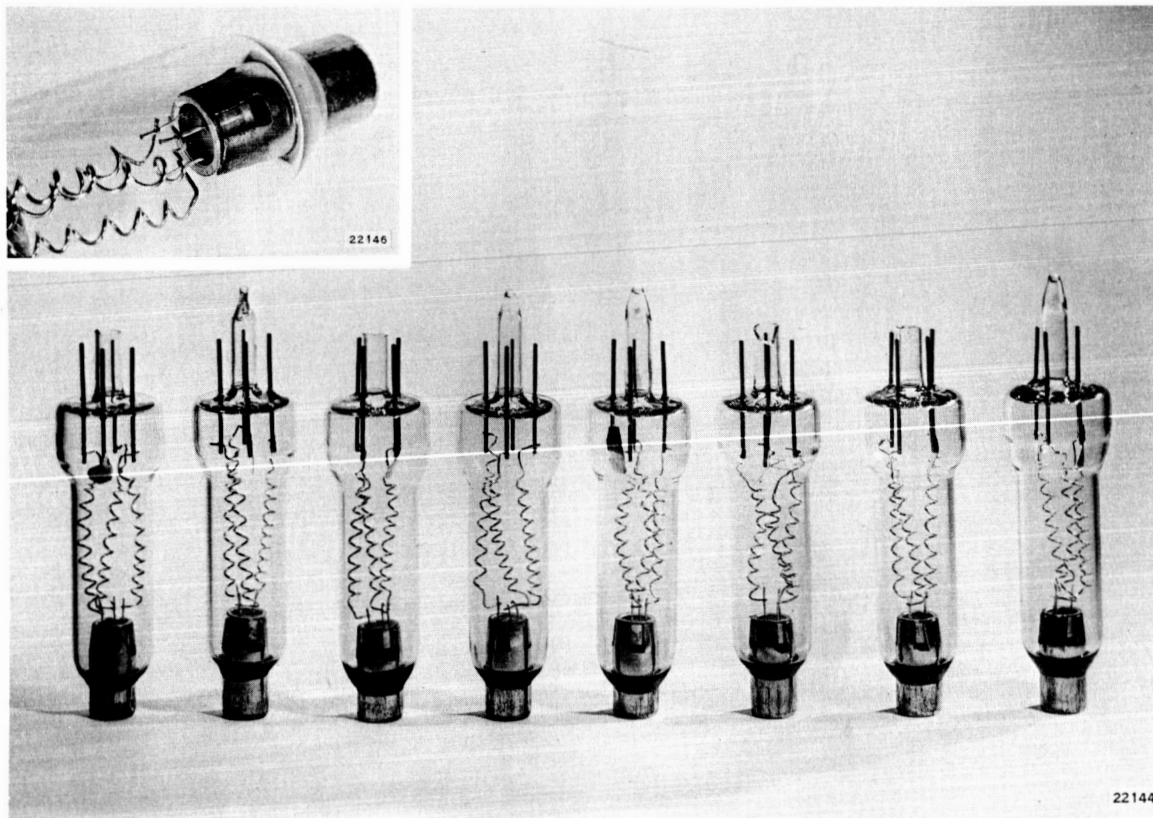


Figure 9 - Ultrahigh Vacuum Fixture for Irradiating Transistors

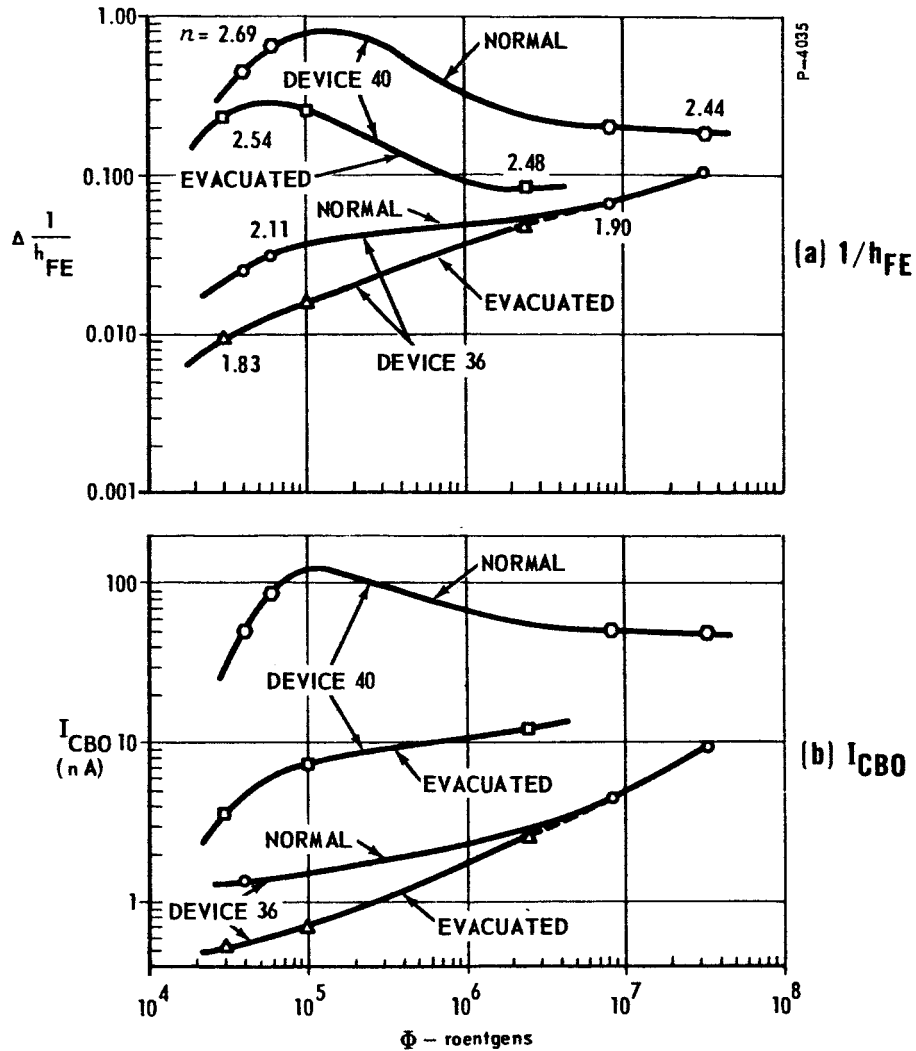


Figure 10 -  $1/h_{FE}$  and  $I_{CBO}$  Versus Dose for Normal and Evacuated Ambients on Devices 36 and 40

Figures 10a and 10b show a comparison of the nitrogen and vacuum ambients for  $V_{CB} = 12$  V during irradiation for Devices 36 and 40. These two devices were selected from a group of 12 which underwent a screening test discussed later in this section. Device 36 was an extremely stable device, the best of the 12 devices tested. Device 40 was very sensitive to ionizing radiation, exhibiting large leakage and gain degradation and high exponential slope constants. Figure 10a is a plot of gain damage

versus exposure time. Both devices exhibited considerable reduction in gain damage due to evacuation; and in both cases exponential slope constants decreased during the irradiation period, indicating recession of a channel. Figure 10b is a similar plot for  $I_{CBO}$ , where the more sensitive unit exhibited a larger improvement due to evacuation. It is interesting to note that for Device 36 the nitrogen ambient runs become asymptotic with the evacuated runs at large doses, indicating that only the early channel term is reduced by a vacuum.

Hogrefe<sup>1</sup> reported on an irradiation-vacuum test accomplished by piercing the encapsulating cans of type 2N1711 transistors aboard an experimental payload prior to placing them in orbit in the Van Allen Belts. Evacuated and normal devices were in space radiation for 100 days ( $\sim 10^5 R$ ) with an active bias of  $V_{CE} = 10V$ ,  $I_C = 0.5mA$ . Due to solar cell degradation this bias had to be removed after 100 days, so that the devices were passive during irradiation for the remainder of the mission. Hogrefe reports that during the first 100 days evacuated units exhibited much less damage than normally encapsulated units,<sup>1</sup> while after several hundred days<sup>14</sup> of passive irradiation the difference in damage between vacuum and gas ambient no longer existed. These data are in basic agreement with those observed for X-rays, where vacuum reduced the early channel component in devices with a reverse collector-base but had little influence on devices irradiated passively.

#### Screening Test

Based on knowledge gained from the X-ray tests, a simple screening procedure was devised. It was designed to compare the susceptibility to



ionizing radiation of  $h_{FE}$  and  $I_{CBO}$  for several transistors of the same type or of different types. To evaluate both  $I_{SRG}$  and  $I_{CH}$  damage components, an irradiation test was chosen, which utilized a reverse-biased collector-base junction (12V). Two data points were taken, the first during early damage buildup ( $\sim 10^5 R$ ) where  $I_{CH}$  dominates, and the second after a large dose ( $> 5 \times 10^6 R$ ) where  $I_{SRG}$  dominates. Data taken at each point consisted of  $h_{FE}$ ,  $I_{CBO}$ ,  $C_{BC}$  and  $C_{BE}$ . This irradiation cycle was followed by a five-hour,  $300^\circ C$  annealing period to return devices to their original conditions.

To evaluate the procedure transistors of types 2N1613 (Fairchild), 2N2222 (Fairchild), ~~2N2222~~ (Motorola), 2N2219A (Motorola), 2N1132 (Texas Inst), 2N2905 (Motorola), and 2N3964 (Fairchild-Planar II) were tested in lots of 12 each. Following annealing, the devices were again subjected to the same screening test to determine if they would repeat their original behavior. Agreement between the first and second tests was good for both n-p-n and p-n-p devices, indicating that radiation screening followed by temperature annealing is very useful in selecting devices for ionizing radiation environments.

All n-p-n types tested exhibited  $h_{FE}$  damage behavior similar to that discussed previously where  $I_{CH}$  dominated at low doses and  $I_{SRG}$  dominated at large doses. All p-n-p types tested did not exhibit this behavior.  $I_{CBO}$  degradation was similar to that for n-p-n; however,  $h_{FE}$  channels did not recede at large doses. Instead damage built up gradually, with a large  $I_{CH}$  component in  $h_{FE}$  at large doses. This component showed no tendency to decrease at doses as high as  $3 \times 10^7 R$ . The model discussion in the following section will attempt to explain this difference.

This simple procedure enables screening of device types and selection of individual transistors which are least susceptible to damage by the ionizing radiation environment to be encountered, either low dose ( $<10^5\text{R}$ ) or high dose ( $>10^6\text{R}$ ). Ionizing radiation screening can be combined with well established bulk damage prediction techniques<sup>15</sup> to select devices for environments possessing the dual threat of surface and bulk damage, such as space radiation, space power and propulsion reactors, and nuclear weapons.

#### DAMAGE MODEL DISCUSSION

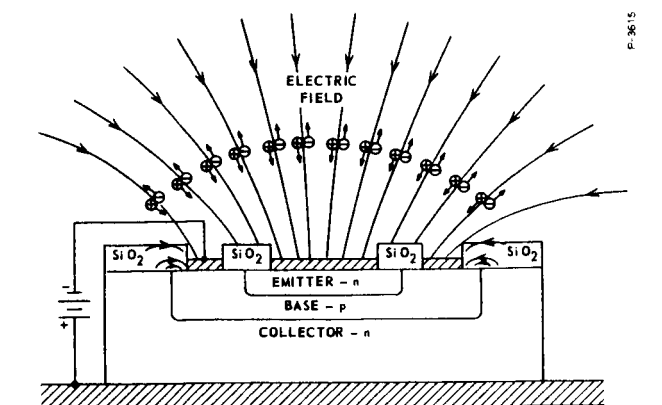
The oxide space charge buildup mechanisms discussed in the introduction have two characteristics in common. Both involve mobile charge carriers, and both require the presence of an electric field either in the surrounding ambient or in the  $\text{SiO}_2$  layer. The following discussion of the model considers two categories of bias conditions: one during irradiation with passive or forward-biased junctions, where no electric fields are produced in the gas ambient; and the second with a reverse bias on at least one of the device junctions, which produces significant electric fields in the gas ambient.

In the first case, where both junctions are either passive or forward-biased, gas ion collection on the oxide surface is unlikely since the ambient has no significant electric field. Charge migration can take place, however, in the  $\text{SiO}_2$  layer directly over a junction, due to the fringing field produced by the junction transition region potential. The polarity of this potential is such that positive mobile charges migrate laterally in the oxide toward the p side of the junction,

and negative charges toward the n side. This type of space charge buildup reduces the silicon surface potential near the junction, which causes the junction transition region to widen at the SiO<sub>2</sub>-Si interface and the surface recombination velocity to increase. The increases in junction geometry and surface recombination velocity enhance the  $I_{SRG}$  component. The high current  $h_{FE}$  component is also enhanced by the base region surface recombination velocity and by the greater likelihood of injection near the surface.<sup>16</sup> The oxide charge migration and resultant junction widening reduce the junction fringing fields, which decelerates the process, eventually producing a saturation condition. Irradiation tests of passive and forward bias n-p-n devices indicate that this process occurs slowly and does in fact produce damage characteristic of  $I_{SRG}$ . Forward bias junctions produce less damage than passive, as would be expected, since the forward bias reduces the junction transition region voltage, which in turn reduces the fringing field in the oxide.

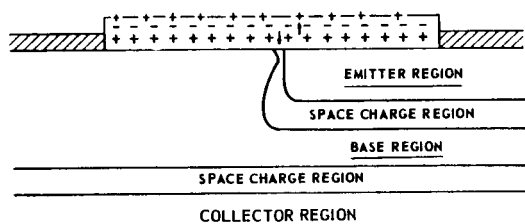
n-p-n transistors irradiated with a reverse bias on the collector-base junction develop an  $I_{CH}$  component in base current which increases rapidly during early radiation exposure, accompanied by an increase in  $C_{BE}$  and an  $\beta$  in excess of 2. Since the collector-base fringing field is too far from the base emitter junction to exert a strong influence, the gas ion model is included in an explanation of this behavior. Figure 11 depicts the model to be discussed.

A reverse collector-base bias produces an electric field in the gas surrounding the device wafer. For n-p-n's this field attracts positively charged gas ions<sup>11</sup> to the SiO<sub>2</sub> surface over the base region (See Figure 11a),



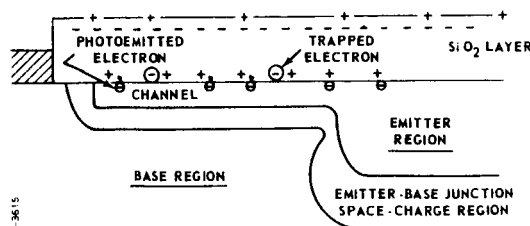
ATTRACTION OF POSITIVE GAS IONS TO BASE AND EMITTER REGIONS  
BY REVERSE COLLECTOR-BASE BIAS

(a)



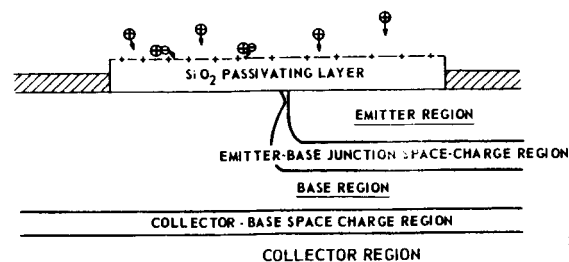
MIGRATION OF IONIZED SPECIES IN THE OXIDE CAUSES A DRIFT  
OF POSITIVE SPACE CHARGE TOWARD THE INTERFACE

(c)



CANCELLATION OF POSITIVE CHANGE IN  $\text{SiO}_2$  LAYER  
PHOTOEMISSION OF ELECTRONS

(e)

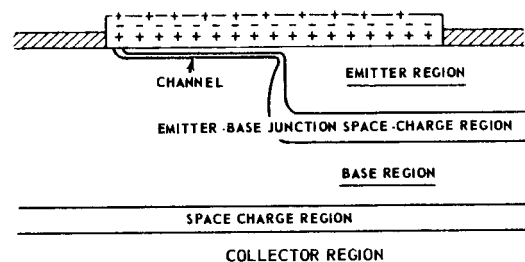


CREATION OF  $\text{SiO}_2$  SURFACE  
SPACE CHARGE BY INTERACTION WITH GAS IONS

(b)

CHARACTERISTICS

1. HIGH CURRENT GENERATION
2. INCREASED JUNCTION AREA
3. INCREASED JUNCTION CAPACITANCE

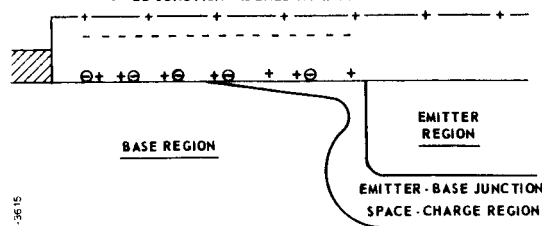


CHANNEL INDUCED BY ACCUMULATION OF POSITIVE SPACE  
CHARGE AT THE  $\text{SiO}_2$ -Si INTERFACE

(d)

CHARACTERISTICS

1. SURFACE POTENTIAL REDUCED
2. SURFACE RECOMBINATION VELOCITY HIGH
3. EB JUNCTION WIDENED AT INTERFACE



RECESSION OF CHANNEL DUE TO CANCELLATION  
OF POSITIVE OXIDE SPACE CHARGE

(f)

Figure 11 - Model for Ionizing Radiation Surface Effects

and the ions give up their positive charge to  $\text{SiO}_2$  surface "sites" by attracting electrons from these sites.<sup>10</sup> (See Figure 11b). This positive space charge over the base region surface can account for the sensitivity of damage to collector-base bias and, if the space charge density is great enough, explain the creation of an inversion layer or channel over the base region. The Fairchild 2N1613 has a base region oxide thickness of from 4000 Å to 6000 Å, and the base surface carrier concentration ranges from  $2 \times 10^{18} \text{cm}^{-3}$  to  $5 \times 10^{18} \text{cm}^{-3}$ . The potential required across the oxide at the onset of inversion for the above dimensions ranges from 22 volts to 54 volts.<sup>13</sup> The voltage due to gas charging the  $\text{SiO}_2$  surface can be no greater than the voltage applied at the collector-base junction. Since  $V_{CB} = 6\text{V}$  produced significant channels, charge migration in the oxide must be included.

Mobile charge species created by ionizing radiation in the oxide will migrate under the influence of the electric field that is created across the oxide by the accumulated  $\text{SiO}_2$  surface charge discussed above. The migrating charge species may be positively charged or negatively charged or both; however, the net effect of either is the same for the transistor base region. Either positive or negative charge migration produces a positive space charge drift toward the  $\text{SiO}_2$ -Si interface (See Figure 11c), which results in an increased electric field in the oxide near the interface and inversion of the p-type base region beneath the interface (See Figure 11d). This space charge buildup model cannot explain the observed behavior of n-p-n devices since it provides no means of removing the channel at large doses. Photoemission of electrons

from silicon across the  $\text{SiO}_2$ -Si interface, as discussed by Williams,<sup>17, 18</sup> explains the elimination of base region channels from n-p-n transistors at large doses. The electron threshold energy for photoemission is 4.22 eV for a p-type surface and 3.05 eV for an n-type surface--energies easily achieved with the ionizing radiation sources of interest. Electrons emitted from the silicon into the  $\text{SiO}_2$  are trapped near the interface, causing a net reduction in the positive space charge over the interface (See Figure 11e). Photoemission is dependent on the electric field at the  $\text{SiO}_2$ -Si interface. The electric field produced by positive oxide space charge over the interface enhances the probability of photoemission into the oxide, while a negative space charge eliminates photoemission. For n-p-n transistors with reverse biased collector-base junctions during irradiation, the net positive oxide space charge drift to the interface over the p-type base region enhances the probability of photoemission into the oxide. At some point, the net positive charge drift to the interface equals the net flow of photoemitted electrons to the interface. As photoemission continues, the positive space charge decreases, which in turn reduces the interface electric field and the channel. Eventually the space charge decreases to a point where the channel disappears (See Figure 11f) and photoemission either ceases or continues at a low rate to replenish electrons drifting toward the oxide surface.

A model similar to that presented above can be proposed for p-n-p transistors with reverse biased collector-base junctions during irradiation.

In this case, negative charge deposited on the oxide surface from the ionized gas causes a net negative space charge drift to the interface over the n-type base region. With the negative space charge, photo-emitted electrons are rejected from the oxide. Any electrons that are trapped in the oxide increase the negative space charge, increasing the channel. Thus it is not surprising that the p-n-p transistors discussed earlier did not recover from the channeling at large doses.

In both n-p-n and p-n-p devices a collector-base channel built up early and decayed at larger doses, affecting  $I_{CBO}$ . This channel was detected by  $C_{CB}$  measurements. Very sensitive p-n-p devices exhibited a characteristic early peak in  $I_{CBO}$  similar to that shown in Figure 7 for Device 8, an n-p-n. The early increase in  $I_{CBO}$  for n-p-n's and p-n-p's is apparently due to a channel from inversion of the p-side of the collector-base junction. This channel recedes at large doses due to photoemission of electrons across the interface, as discussed in the  $h_{FE}$  model above. The remaining  $I_{CBO}$  damage at large doses is either channel current from inversion of the n-side of the junction or  $I_{SRG}$  from fringing field effects similar to those discussed for passive and forward biased junctions.

## CONCLUSIONS

An investigation has been made of the effects of ionizing radiation on transistor  $I_{CBO}$  and  $h_{FE}$  with measuring conditions and electrical bias during irradiation as variables. Two current components were identified that affect  $I_{CBO}$  and  $h_{FE}$  at low levels: surface channel current and surface space charge region recombination-generation current. To explain variations in both  $h_{FE}$  and  $I_{CBO}$  for both n-p-n and p-n-p transistors, a model has been proposed which includes the effects of bias during irradiation. Based on test results and the model, a procedure was devised consisting of an irradiation screening test followed by temperature annealing, which enables selection of transistor types and individual transistors which are least sensitive to ionizing radiation.

*AUTHOR*

## ACKNOWLEDGMENTS

The authors wish to thank J. Brosko, L. Laniewski, T. Burt, and G. Ralston for their assistance in performing irradiation tests and Dr. R. K. Mueller for valuable discussions concerning the model.



#### REFERENCES

1. A. F. Hogrefe, "Design and Packaging to Survive an Extended Mission in the Natural and Artificially Trapped Belts of Near Space," National Electronic Packaging Conference, New York, Summer 1964
2. H. L. Hughes, "Surface Effects of Space Radiation on Silicon Devices," IEEE Transactions on Nuclear Science, NS-12, 53-63, December 1965
3. J. C. Peden et al, "Radiation Surface Effects in Silicon Planar Transistors," presented at IEEE Nuclear Radiation Effects Conference, Seattle, 1964
4. A. Stanley, "Space Radiation Effects on High Gain Low Current Silicon Planar Transistors," MIT-LL Group Report 1965-11 under Contract AF 19(628)-5167, February 1965
5. A. Stanley, "Effects of Electron Irradiation on Metal-Oxide-Semiconductor Transistors," Proceedings of IEEE, 53, 627-628, June 1965
6. A. J. Speth and F. F. Fang, "Effects of Low Energy Electron Irradiation on Si-Insulated Gate FETs," Applied Physics Letters, 7, 145-146, September 1965
7. E. Kooi, "Influence of X-ray Irradiations on the Charge Distributions in Metal-Oxide-Silicon Structures," Philips Research Reports, 20, 306-314, 1965
8. C. D. Taulbee, D. L. Nelson, B. G. Southward, "Radiation Effects in Electronics," ASTM Special Technical Publication, 384, 121-148 October 1964
9. A. S. Grove and E. H. Snow, "A Model for Radiation Damage in Metal-Oxide-Semiconductor Structures," Proceedings of IEEE, 54, 894-895, June 1966
10. P. J. Estrup, "Surface Charge on Silicon Inducted by Ambient Ionization," Solid State Electronics, 8, 535-541, 1965
11. D. S. Peck et al, "Surface Effects of Radiation on Transistors," Bell System Technical J, 42, 95, January 1963
12. C. T. Sah, "Effect of Surface Recombination and Channel on P-N Junction and Transistor Characteristics," IRE Transactions on Electron Devices, ED-9, 94-108, January 1962

13. D. J. Fitzgerald and A. S. Grove, "Mechanisms of Channel Current Formation in Silicon P-N Junctions," presented at Fourth Physics of Failure Symposium, Chicago, November 1965
14. Private communication, D. L. Nelson and A. Hogrefe, July 1966
15. M. Frank and F. Larin, "Effect of Operating Conditions and Transistor Parameters on Gain Degradation," IEEE Transactions on Nuclear Science, NS-12, 126-133, October 1965
16. V. G. K. Reddi, "Injection of Minority Carriers at a Field-Induced Junction Near the SiO<sub>2</sub>-Si Interface," IEEE Transactions on Electron Devices, ED-13, 381, March 1966
17. R. Williams, "Photoemission of Electrons from Silicon Into Silicon Dioxide. Effects of Ion Migration in the Oxide," Journal of Applied Physics, 37, 1491-1494, March 1966
18. R. Williams, "Photoemission of Electrons from Silicon Into Silicon Dioxide," Phys Rev, 40, A569-A575, October 1965